Drug Development and Industrial Pharmacy, 33:1030–1039, 2007

ISSN: 0363-9045 print / 1520-5762 online
DOI: 10.1080/03639040601180143

informa
healthcare

Purification of PEGylated Nanoparticles Using Tangential Flow Filtration (TFF)

Gautam Dalwadi and Vivian Bruce Sunderland

School of Pharmacy, Curtin University of Technology, Bentley Campus, Bentley, Perth, Western Australia, Australia

A tangential flow filtration system was evaluated to purify PEGylated nanoparticles. Two widely used surfactants, PVA and sodium cholate were efficiently removed from an empty nanoparticles suspension using the proposed system. During drug loading, surfactant (PVA) was observed to be entrapped within the core of the nanoparticle to a higher extent, hence was purified at a comparatively slower rate. The presence of dextran sulfate enhanced the drug loading but also resulted in reduced purification rate; this was described by the hypothesis of PVA inclusion within the core of the nanoparticles. Practically, it was possible to correlate the slow purification rate of PVA to its reduced filtration flow during the purification of the empty and loaded nanoparticles containing dextran sulfate. Indirectly, this system was capable of revealing the influence of an excipient and drug on the nanoparticle surface.

Keywords PEGylated nanoparticle; purification; TFF

INTRODUCTION

Preparation of poly (D,L-Lactide co-glycolide) (PLGA) based nanoparticles normally involves the use of a large amount of surfactant. Various surfactants have been used in the preparation of nanoparticles from PLGA based copolymers, however polyvinyl alcohol (PVA) is commonly used due its effectiveness in obtaining nanoparticles and stabilising properties compared to other surfactants (Murakami, 1999; Vandervoort, 2002). However, when the nanoparticles are formulated for parenteral use, the presence of surfactants is undesirable due to their potential toxicities. PVA is generally used in concentrations of 3–5% in nanoparticle formulations, at this level it produces anemia and infiltrates in various organs and tissue, beside its proven carcinogenicity on repeated use (Youan, 2003). Its presence could extensively damage the red blood cells (Kim, 2005) and also affects the cellular intake (Sahoo, 2002). Therefore, the use of PVA is restricted in parenteral formulations. Considering this fact, there is a need for the development of a purification method that can remove or reduce the level to a reasonable limit in such formulations. Alternatively, other biocompatible surfactants may be used that effectively produce nanoparticles (Mu, 2002). Additionally, such surfactants can be grafted on to the PLGA backbone to obtain a copolymer as a new entity that may required little or no additional surfactant to form nanoparticles (Dailey, 2005). However the use of entirely novel copolymers requires a whole range of toxicological testing in order to consider them for human pharmaceuticals. This could be more costly than developing and validating a purification process to remove undesirable surfactant/impurities from nanoparticles prepared from copolymers that are already acceptable for pharmaceutical use.

Polyethylene glycol (PEG) is an approved safe excipient widely used in pharmaceuticals. Its copolymerisation with glycolide and lactide monomers gives rise to another category of novel copolymers, which are equally regarded safe for pharmaceutical use. The PEGylated PLGA copolymer provides many additional in vitro as well as in vivo advantages over conventional PLGA.

A PEGylated PLGA copolymer is reported to form nanoparticles by a common process that required relatively less PVA, compared to that of nonPEGylated. This is due to its hydrophilic stealth provided by the presence of PEG that reduces the interfacial tension during nanoparticle formation. The amount of PVA to be utilized to form nanoparticles is dependent on the percentage composition of PEG on the copolymer. Despite grafting 15–20% $PEG_{2000–5000}$ on to PLGA (35–50,000 MW), 0.5–0.6% PVA is still required to obtain nanoparticles with a core and shell structure (Gref, 1995). This level is undesirable when the particles are designed to be administered intravenously especially for brain targeting of drugs.

Alternatively, the use of sodium cholate and other bile salt based surfactants in the concentration range from 10 to 20 mM

Address correspondence to Gautam Dalwadi, School of Pharmacy, Curtin University of Technology, Bentley Campus, Bentley, Perth, Western Australia, 6102, Australia. E-mail: gdalwadi@hotmail.com

is also reported in the formulation of nanoparticles from PEGylated-PLGA copolymers (Gref, 1995). This level of bile salts in the nanoparticle formulation is toxic via the intravenous route. Generally, sodium cholate is tolerable by intestinal cells when given orally but is reported to damage cell membranes by solubilization of membrane lipid and protein at concentrations of 1 to 20 mM when delivered intravenously (Child, 1986). Therefore, their removal from the formulation becomes essential if the particles are delivered via the intravenous route, and there is a need for developing an industrially scalable purification process to achieve this purpose.

Traditionally, high speed centrifugation at 50,000–300,000 × *g*-forces up to 3 h is commonly used to separate the surfactants from the nanoparticles (Govender, 1999; Niwa, 1993; Riley, 1999). This also leads to the formation of pellets which are generally difficult to redisperse due to aggregate formation (Chiellini, 2003). Use of lower g-forces can be adopted to avoid aggregate formation, however lower than 50,000 × *g* force conditions during centrifugation has resulted in incomplete separation of the submicron particles from the supernatant especially for particle sizes less than 100 nm. In the current experiment, the use of PEGylated PLGA resulted in a very small nanoparticles (80–120 nm) compared to that of nonPEGylated. This did not resolve from the free surfactants under the proposed ultracentrifugation conditions therefore an alternative process was developed to purify the nanoparticles from excess surfactant and free drug.

Recently, ultrafiltration techniques have been expanded for the separation of a variety of macromolecules from complex matrices. Tangential flow filtration (TFF) is a unit operation that is inherently used to separate solutes differing by more than 10 fold in their size (Reis, 1997); the application is widely exploited in the area of biotechnology, mainly in purifying cell, virus and bacterial proteins (Charcosset, 2006). With the growth of nanotechnology and its application in the biopharmaceutical field, there is an expanding application to process nanosized pharmaceutical colloids. A successful use of diafiltration and TFF has been demonstrated in nanoparticle purification from excess surfactants and residual solvent (Limayem, 2004; Tishchenko, 2003). The use of TFF is not only limited to polymeric nanoparticles, but has been successfully extended to separation of various sized gold nanoparticles from small impurities (Sweeney, 2006) and in the field of liposomes as well as cationic solid lipid nanoparticles (Guichardon, 2005) to remove surfactants to minimize toxicity (Heydenreich, 2003).

In our laboratory we have successfully developed the TFF system to remove PVA from PLGA based nanoparticles (Dalwadi, 2005). In the current study, this technique is further explored to purify PEGylated PLGA based nanoparticles with quantitative monitoring of the most widely used surfactants PVA and sodium cholate.

MATERIAL AND METHODS

Materials

Polyvinyl alcohol (PVA) (80–89% hydrolyzed, MW 9000–10,000, Sigma Aldrich [St. Louis, MO]), Minimate™ capsule with Omega™ 300 K membrane (Lot # 3086E003) purchased from PALL Scientific (East Hills, NY). Dextran sulfate (MW 5000, Lot # K30054789 O, Sigma Aldrich), Loperamide HCl (99% pure, Lot # 103K0611, Sigam Aldrich), Sulfuric acid (AR grade, Lot # K25120855, Mallincordt). Polyethylene glycol (monomethyl ether) (99% pure, Lot # 44931/1, Fluka, Germany). Glycolide monomer (Purasorb^{G}, 99.9% pure, Lot # 0305000324), D,L-Lactide monomer (Purasorb^{D}, 99.9% pure Lot # 0310000164) purchased from PURAC International, Holland. Stannous octoate (95% pure, Lot # 102K0104, Sigma Aldrich). Sodium cholate (99% pure, Lot # 092K0123, Sigma Aldrich). Ultra pure water (<6 μS) prepared from a Milli-Q purification system was used in all experiments.

Synthesis and Characterization of mPEG-PLGA a Co-Polymer

Synthesis and Characterisation

The synthesis of monomethoxy poly(ethylene glycol) – poly (D,L-lactide-co-glycolide) (mPEG-PLGA) co-polymer was performed via a ring opening polymerisation (Beletsi, 1999; Gilding, 1979). Briefly, 4 g of D, L-lactide, 4 g of glycolide and 4 g of monomethoxy poly (ethylene glycol) (mPEG) were mixed and heated at 140°C under an inert atmosphere (nitrogen) for 6 hr in the presence of 0.085 g of stannous octoate as a catalyst. After polymerization the melt was dissolved in minimum dichloromethane and precipitated from excess methanol several times. The purified copolymer was subjected to thermal characterization using modulated differential scanning calorimetry (mDSC) (TA instrument, Model Q100) to determine a glass transition temperature T'_g from second heating scan which was found to be 24.58°C. Relative molecular weight and polydispersity of the copolymer were determined by organic solvent based gel permeation chromatography (GPC), which were found to be 35,974 with polydispersity 2.5 relative to the polyethylene glycol standards. The polymer composition was determined using the intensity ratio of methylene (-CH_2-) of ethylene oxide proton shift at 3.6 ppm, to the shift at 4.78 ppm for methylene (-CH_2-) protons of the glycolide and the shift at 5.15 and 1.60 ppm of methine (-CH-), as well as (–CH_3) protons of D, L-lactide respectively in H^1 NMR spectrum. (Beletsi, 1999; Du, 1995). From the intensities of these protons, the weight ratio of $mPEG_{2000}$:Lactide:Glycolide was found to be (17.4:73.0:11.2) in composition. The identity and the proof of the ring opening polymerization was confirmed using the vibrational spectra of the monomers and copolymer. In Raman spectra, the carbonyl (⟩C = O) stretching vibration of glycolide and D, L-lactide monomers appeared at 1768.7, 1791.33, and 1764.00 cm^{-1} frequencies, which

disappeared from the final Raman spectrum of the copolymer, instead appeared as a wide non-symmetrical band at 1760.2 cm^{-1} with 1737.00 cm^{-1} as a shoulder which indicated the vibration of the (⟩C = O) of ester (–COO), this confirmed opening of the lactonic ring followed by polymerization. (Bhatt, 1964; Durig, 1963, 1968; Kister, 1992). In Raman spectra, the ring vibration modes with max. at 794.01 cm^{-1} with shoulder at 745.36 cm^{-1} appeared for glycolide, with doublets at 790.77 cm^{-1} and 768.10 cm^{-1} for D, L-lactide. These were not observed in the final spectrum of copolymer, instead, a new intense line occurred at 868.0 cm^{-1} with a shoulder at 893.58 cm^{-1} attributed to stretching of ⟩C-COO, which indicated another characteristic of ring opening polymerization (Bhatt, 1964; Durig, 1963, 1968; Kister, 1992). In the IR spectra of individual monomers, a broad and large band at 1760 cm^{-1} was assign to -C = O stretching, squeezed into a strong band with comparatively less band width at 1764 cm^{-1} after polymerization. The IR group frequencies at 3648.05 and 3506.99 cm^{-1} as a small to medium band in the spectrum confirmed the presence of free -OH or –COOH terminal groups of co-polymer, however the intensities of these peaks were reduced compared to that of the IR spectra of $mPEG_{2000}$, due to incorporation of a hydrophobic polyester segment into mPEG that reduced the extent of hydrogen bonding. In the final copolymer, three medium IR bands at 2995.7, 2947.51, and 2881.12 cm^{-1} mainly arise from C-H stretching of sp^3 hybridized carbon from ethylene, lactide and glycolide units (Beletsi, 1999; Gilding, 1979). The copolymer with these properties was used in all experiments.

Preparation and Characterisation of Empty and Drug Loaded Nanoparticles

Preparation of Nanoparticles Using Sodium Cholate as a Surfactant

An o/w techniques was adopted to prepare empty nanoparticles. A total of 100 mg mPEG-PLGA was dissolved in 8 ml of acetone and added drop wise to 50 ml 12 mM sodium cholate solution as a continuous phase, and stirred over a period 7.5 hr, this provided a nanoparticle suspension on evaporation of acetone.

To prepare empty nanoparticle, a double emulsion method (w/o/w) was adopted from (Olivier, 2002). 125 mg of mPEG-PLGA was dissolved in 5 ml DCM to that 0.25 ml of pure water was added, followed by high speed homogenisation for 1 min. This primary emulsion was added to 10 ml of 1% sodium cholate solution under constant homogenisation at 10,000 rpm (Diax 900 Heidolph). Once the addition was complete, the solution was allowed to homogenise for 2.5 hr at ambient conditions. The volume of the suspension was made to 50 ml using 0.5% sodium cholate solution. The DCM was rotary evaporated. The sodium cholate content of the preparation was measured as stated below.

Preparation of Nanoparticles (o/w Method) Using PVA as a Surfactant

The drug loaded nanoparticles were prepared from 200 mg of mPEG-PLGA co-polymer dissolved in 6 ml of 2 mg/ml Loperamide HCl solution in acetone; a further 4 ml of acetone was added for solubilisation followed by addition of 0.025 ml DCM. To this organic phase 0.3 ml of 20 mg/ml solution of dextran sulfate (MW 5000) was added. The entire organic phase was added drop wise to 60 ml 0.6% PVA solution. The solution was stirred for 7.5 hr at ambient conditions.

The empty nanoparticles with dextran sulfate were prepared by excluding loperamide HCl in acetone followed by adopting similar preparation conditions mentioned above.

The empty nanoparticle without dextran sulfate was prepared by excluding both, the dextran sulfate and the drug in the preparation.

Particle Size and Zeta Potential Measurement

Nanoparticle size and a zeta potential were measured on Zetasizer 3000HS (Malvern Instrument, UK). The particle size was measured by photon correlation spectroscopy (PCS) at 25°C with a detection angle of 90°. The average mean size Z was derived from the raw data using a Zetasizer HS software using cumulative analysis mode. The zeta potential was determined by laser doppler anemometry. This procedure was performed on the particle before and after purification.

Quantification of Surfactant and Drug

Quantification of Sodium Cholate

The method was adopted from (Mosbach, 1954). Briefly, accurately weighed 11 mg sodium cholate was dissolved upto 100 ml water. Aliquots of 0.2 to 4.0 ml were pipetted accurately in to a 5 ml volumetric flask. Each solution were dried under vacuum at 40°C for 2 hr. Freshly prepared 5 ml of 65% w/v sulfuric acid was added to each dried sample. Absorbance of each solution was measured at 319 nm using a UV-Vis spectrophotometer (Shimadzu). The concentration of sodium cholate in 5 ml sulfuric acid solution vs. absorbance at 319 nm was plotted as a calibration curve over a concentration range from 20.96 to 419.32 μg/ml ($y = 0.0062x + 0.0837$, $R^2 = 0.9992$).

Assay of Sodium Cholate in Nanoparticle Suspension

A 1 ml nanoparticle sample was centrifuged in eppendorf tubes at 13,400 rpm for 20 min. A 0.05 ml of supernatant was dried under vacuum at 40°C for 2 hr in a separate vial followed by addition of 65% w/v sulfuric acid solution, which was measured for absorbance at 319 nm by UV-vis spectrophotometry. The amount was calculated using the calibration curve mentioned in the previous section. This method was found to be accurate with in 100 ± 2.23% $n = 3$. This was determined by adding known amounts of the sodium cholate into the purified nanoparticle suspension assayed by the proposed method.

Quantification of PVA

The colorimetry assay for PVA was adopted from (Finely, 1961). Briefly, a standard curve was prepared by appropriate dilution of 2 mg/ml PVA stock solution to obtain a concentration range from 0 to 25 μg/ml. To each fraction of stock solution 5 ml of water, 3 ml of 4% boric acid, and 0.6 ml of 0.1 N iodine solution were added, finally 10 ml was made up with water. This generates a complex between boric acid and PVA which has a green colour in the presence of iodine solution, which provided optimum absorbance at 690 nm by UV-Vis spectrophotometry. This method was found to be linear over the stated concentration range ($y = 0.0221x + 0.0364$, $R^2 = 0.9993$), with an accuracy of 100.30 ± 4.37, $n = 3$ and was also specific to quantify PVA in the nanoparticle matrix.

Assay of PVA Content in Nanoparticle Suspension

A volume of 0.5 ml of nanoparticle suspension was centrifuged at 13,000 rpm for 20 min, then 0.05 ml of supernatant was diluted with 5 ml of water, 3 ml of 4% boric acid solution and 0.6 ml 0.1 N iodine solution finally adjusted to 10 ml using water. The absorbance was measured at 690 nm by UV-Vis spectrophotometry. The relevant amount of PVA was calculated from the calibration curve generated previously.

HPLC Assay of Loperamide HCl

A HPLC method was developed using a reversed phase C_{18} column and a Waters HPLC system comprised of dual wavelength UV detector, dual piston pump, autosampler controlled by Breeze™ software. Loperamide HCl was quantified over a concentration range 2 to 300 μg/ml ($y = 93400x + 8662$, $R^2 = 0.9999$) with accuracy of 94.35 ± 7.63%, ($n = 8$). The mobile phase was 65:35 acetonitrile:buffer containing 20 mM Tri-ethyl amine (TEA), 20 mM phosphate buffer at pH = 5.0, and a flow rate of 0.5 ml/min, with detection wavelength 220 nm. The pK_a value of loperamide HCl is 8.6, therefore under the proposed conditions of the mobile phase it remained in the ionized form. A similar pH (5–5.5) was also maintained in the dispersed phase of the nanoparticle preparation, therefore the current HPLC method and its calibration data was performed using the salt form of the loperamide.

The dried recovered mass (100 mg, accurately weighed), after each purification was digested in 10 ml of 2% methanolic KOH by sonicating for 5 min, a clear fraction was separated by centrifugation (10,000 rpm for 10 min), and loperamide HCl content was determined after 10 fold dilution with mobile phase followed by the HPLC analysis discussed previously.

Purification of Empty and Drug Loaded Nanoparticles by Tangential Flow Filtration (TFF)

The TFF system was set up as shown in Figure 1, adopted from Dalwadi, 2005. The nanoparticle suspension was purified at 10 and 20 psi transmembrane pressure (TMP) on a TFF system which comprised of Minimate™ fabricated with Omega™ 300K membrane (PALL Scientific). Concentrated mode was adopted for purification, where the nanoparticle suspension was circulated through the TFF system using a peristaltic pump back to a reservoir until it concentrated to the minimum possible volume then followed by additional washes by adding purified water in to the reservoir to allow efficient removal of the surfactants.

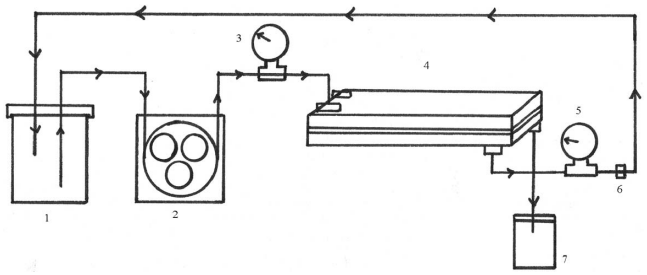

FIGURE 1. Components of the schematics of TFF (Adopted from Dalwadi, 2005). (1) Sample reservoir (2) Peristaltic pump-1 (3) Feed Pressure gauge (4) Minimate™ 300 K (5) Transmembrane pressure gauge (6) Screw clamp valve (7) Filtrate collector.

On starting purification, a 50 ml nanodispersion was processed in concentrated mode until it concentrated to less than 10 ml, at this stage 30 ml of water was added to the reservoir to provide washing; the filtrate was collected again until retentate volume again concentrated to less than 10 ml. Thus, two washes were performed in the case of the nanoparticles containing sodium cholate as surfactant. This purification was performed only on the empty nanoparticles at 10 and 20 psi transmembrane pressures. In the case of the nanoparticles containing PVA, the purification was also commenced with 50 ml with a total of three additional washes to remove the excess PVA. This was performed only at 20 psi on the empty as well as drug loaded nanoparticles.

During the purification, each filtrate fraction obtained from the filtrate port was measured for its volume and the time to collect it. This was followed by measurement of the drug and surfactant in the case of the loaded particle purification and only surfactant in the case of empty nanoparticles using the relevant quantitative methods discussed previously. The filtrate flow rate (ml/min) vs. cumulative time (hr) was plotted for the flow rate data obtained from triplicate experiments of each case, and mean flow rate ± standard deviation for each case was calculated by excluding the initial five time point readings from the average plot. The mean values obtained were statistically compared using p values generated from one way ANOVA with Scheffe's post hoc test.

From the surfactant and drug analysis data generated during triplicate experiments of each case, cumulative % surfactants and cumulative % free drug vs. cumulative time (hr) were plotted

for each case. Their trends were assessed in comparison with the flow rate trend. From the mean purification curve, slope values were obtained to estimate purification rates.

The drug loaded nanoparticles were recovered after the third wash during purification when the dispersion volume was concentrated to 10 ml. Air was pushed into the device and the retentate was collected into preweighed empty containers, then the contents were lyophilized followed by drug analysis by HPLC to confirm encapsulation efficiency.

RESULTS AND DISCUSSION

Purification of Nanoparticles Containing Sodium Cholate as a Surfactant

The nanoparticles prepared by o/w techniques using sodium cholate resulted in small particle size values of less than 40 nm. This was overlapped with the pore size distribution of the TFF membrane. The purification of the first batch was observed to be efficient but subsequently it blocked the TFF membrane (data not presented) during purification hence reproducibility was not achieved. Therefore, w/o/w techniques were adopted to obtain a desired particle size, this provided a larger particle size distribution (290.5 ± 13.4 nm, $n = 3$, Table 4) than the membrane pore size (40 nm). This allowed complete retention of nanoparticles without blocking of the membrane and provided absolute resolution from surfactant.

The purification rate of sodium cholate was faster at 20 psi compared to that at 10 psi. Initially, sodium cholate was removed in a linear relationship at a rate of 240.96%/hr, this slowed due to progressive removal of the sodium cholate and extra water washes causing dilution in the reservoir. Later phases of the purification curve showed a logarithmic fit that showed the sodium cholate removal rate at 29.61%/hr. This was remarkably lowered compared to the purification rate obtained from the initial phase of the curve and indicated that the purification process was near completion (Figure 2). Thus, at 20 psi, in less than 0.5 hr total 94.99 ± 1.26%, $n = 3$ sodium cholate was removed. The major portion (73.00 ± 6.25% $n = 3$) was removed in the filtrate with only 2.90 ± 2.03% $n = 3$ remained associated with the nanoparticles, while 24.10 ± 7.92%, $n = 3$ was estimated to adsorb onto the membrane (Table 1) that was further washed away during the conditioning steps between the purification of two subsequent batches.

A similar trend was observed at 10 psi, where sodium cholate was removed at 168.61%/hr initially, and at 28.60%/hr towards the end of the purification curve. However, at 10 psi, 93.86 ± 0.19% $n = 3$ was purified within 0.75 hr which was slower compared to that at 20 psi. The major portion (71.94 ± 5.60% $n = 3$) was removed in the filtrate, with 4.92 ± 1.69%, $n = 3$ remained associated with the nanoparticles. The remainder 23.14 ± 5.30%, $n = 3$ was estimated to adsorb onto the

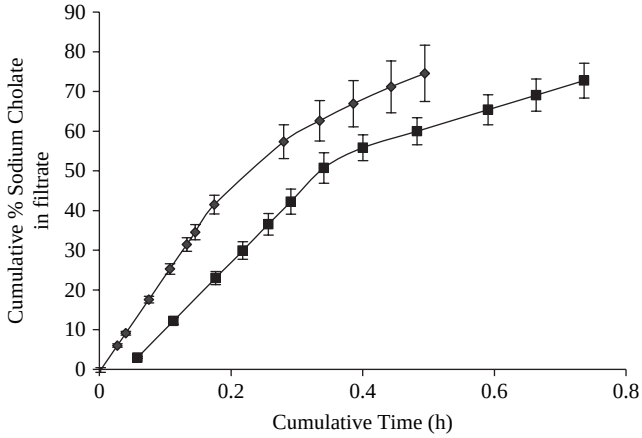

FIGURE 2. Impact of transmembrane pressure on removal of sodium cholate from the nanoparticle formulation. -✦- 20 psi. -■- 10 psi.

TABLE 1
Distribution of Sodium Cholate During Purification by Tangential Flow Filtration (TFF)

	Percentage of Sodium Cholate Distribution (Mean ± *SD*, $n = 3$)				
TMPs (psi)	Before Purification[a]	Loss in Filtrate[b]	Left on Particles (After Purification)[c]	Adsorbed on the Membrane[d]	Total Purified[e]
10	98.78 ± 1.50	71.94 ± 5.60	4.92 ± 1.69	23.14 ± 5.30	93.86 ± 0.19
20	97.89 ± 3.29	73.00 ± 6.25	2.90 ± 2.03	24.10 ± 7.92	94.99 ± 1.26
Sig. (p) (10 vs. 20 psi)	–	$p = 0.838$	$p = 0.256$	$p = 0.870$	$p = 0.810$

TMPs is transmembrane pressures.
SD is standard deviation.
$p < 0.05$ is significant, $p > 0.05$ is not significant, obtained from one way ANOVA test.
[a]assayed.
[b]assayed.
[c]assayed.
[d]estimated {100 – (b + c)}.
[e]estimated (a – c).

membrane (Table 1), that was washed away further with conditioning steps between the purification of two subsequent batches. The slow purification rate at 10 psi compared to that at 20 psi was anticipated and can be further explained by the higher filtration flow rate at 20 psi (Figure 3). In Figure 3, at the commencement of purification, filtrate flow rate progressively fell from 4.00 to 2.63 ± 0.06 ml/min for 20 psi and from 3.00 to 1.89 ± 0.04 ml/min at 10 psi. The overlap of the flow rate values in Figure 3 contributed to the initial dilution of the nanoparticle dispersion by the held back water volume (approximately 15–20 ml) within the TFF system that induced changes in the viscosity and dynamics of the flow until it completely replaced the held back water. This took awhile to stabilize the filtration flow rate. After complete replacement of the nanodispersion throughout the TFF cassette, the filtration flow rate remained stabilized at 2.63 ± 0.06 ml/min and 1.89 ± 0.04 ml/min for 20 and 10 psi, respectively with significant difference *(p* = 0.000, Table 5).

After purification, less than 7% of sodium cholate remained associated with the nanoparticles recovered at both TMPs, with no significant difference (p = 0.256) in the residual amount (Table 1). These results are in agreement with the finding of (Gref, 1995), who reported an almost similar level of sodium cholate association with the nanoparticles after purification. Similarly, the amounts of surfactant loss in the filtrate, adsorbed on the membrane and the total purified were not significantly (p = 0.838, 0.870, 0.810) different at 10 and 20 psi (Table 1). This suggests that only the rate of removal was different during the purification at two different TMPs. The particle size also remained unaffected after removal of sodium cholate during purification at two different TMPs (Table 4).

Purification of the Nanoparticles Containing PVA as a Surfactant

Purification of the PVA containing empty nanoparticles without dextran sulfate was observed at the rate of 165.03%/hr at 20 psi. This was followed by a slower purification rate at 39.91%/hr towards the end portion of the purification curve due to progressive removal of PVA and potential dilution caused by additional water washes (Figure 4). At this rate, a total of 108.42 ± 3.67%, n = 3 of PVA was removed from the nanoparticles, with 5.40 ± 3.0% PVA left on the nanoparticle, while 103.02 ± 4.10%, n=3 PVA was found in the filtrate with minimal adsorption estimated on the TFF membrane (Table 2). This indicates that in the case of the empty nanoparticles without dextran sulfate PVA was removed efficiently. However, the drug loaded nanoparticles containing dextran sulfate, surprisingly purified at a very slow rate compared to the previous one (Figure 4). In Figure 4, the curve was arbitrarily divided into three equal segments to calculate the slope values from their linear fit equation to follow the purification rates of PVA at different time points on the curve; this was found to progressively decrease from 58.34 to 22.41%/hr towards the end of the process. Despite 1.5 hr purification time, only 69.35 ± 2.50%, n = 3 of PVA was purified with minimal surfactant adsorption on the membrane (4.85 ± 1.36%, n = 3). This indicates that most of the purified PVA was lost in the filtrate (64.50 ± 3.84%, n = 3). At the end of purification, almost 30.64 ± 2.50%, n = 3 PVA was found to be associated with the nanoparticles (Table 2). This value was significantly higher (p = 0.000) than the amount of PVA associated with the empty nanoparticles without dextran sulfate. A high level of PVA association was also reported by (Gref, 1995). At the same time, the filtration flow rate of the empty nanoparticles without dextran sulphate was significantly higher (p = 0.039, 0.005) compared to the empty and loaded nanoparticle with dextran sulphate (Table 6, Figure 6).

To confirm the impact of the dextran sulfate on the purification behavior of the PVA, another set of experiments was

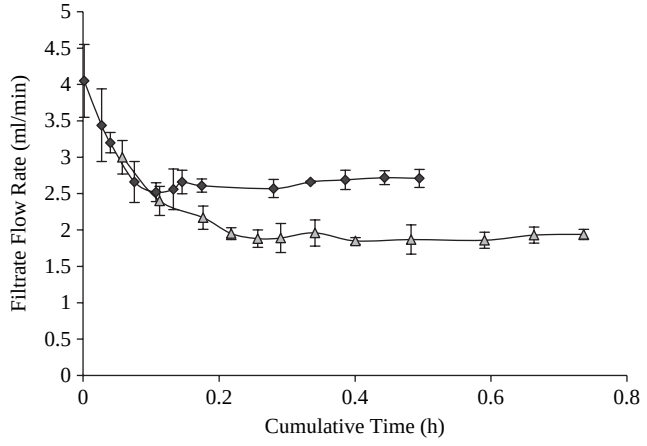

FIGURE 3. Impact of transmembrane pressure on the filtrate flow rate -✦- 20 psi. -Δ- 10 psi.

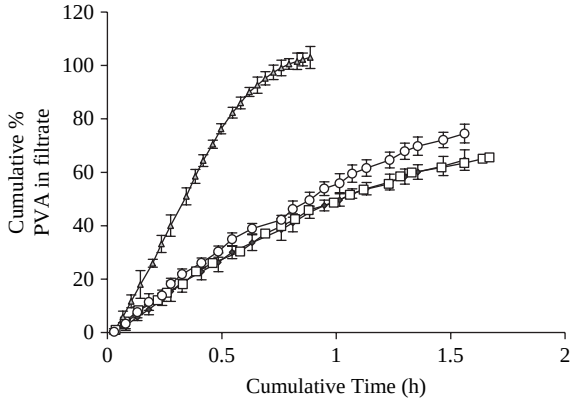

FIGURE 4. Removal of PVA from PEGylated nanoparticles. Impact of dextran sulfate on purification trend. -Δ- Empty nanoparticle without dextran sulfate (n = 3), -✦- Loperamide HCl loaded nanoparticle with dextran sulfate (n = 3), -□- Empty nanoparticle with dextran sulfate (n = 1). -❍- Loperamide HCl loaded nanoparticle without dextran sulfate (n = 3).

TABLE 2
Distribution of PVA During Purification by TFF

Percentage of PVA Distribution (20 psi TMPs) (Mean ± *SD*)					
Formulations	Before Purification[a]	Loss in Filtrate[b]	Left on the Particle (after purification)[c]	Adsorbed on the Membrane[d]	Total Purified[e]
Empty without DS (n = 3)	100.30 ± 4.30	103.02 ± 4.10	5.40 ± 3.0	3.16 ± 5.47	94.90 ± 7.30
Loaded without DS (n = 3)	102.12 ± 3.51	74.52 ± 3.52	22.53 ± 5.26	2.56 ± 4.50	79.59 ± 1.75
Loaded with DS (n = 3)	105.37 ± 4.42	64.50 ± 3.84	30.64 ± 2.50	4.85 ± 1.36	74.72 ± 1.90
Empty with DS (n = 1)	102.50	65.49	31.56	5.02	70.94

DS means dextran sulfate.
SD is standard deviation.
[a]assayed.
[b]assayed.
[c]assayed.
[d]estimated {100 – (b + c)}.
[e]estimated (a – c).

TABLE 3
Distribution of Loperamide HCl During Purification by Tangential Flow Filtration

Percentage of Loperamide HCl Distribution (20 psi TMPs, Mean ± *SD*, n = 3)						
		Left within Nanoparticles				
Formulation	Loss in Filtrate[a]	Expected[b]	Assayed[c]	Sig. (p) b vs. c	Adsorbed on Membrane[d]	Total[e]
Loaded without DS	44.15 ± 1.88	55.50 ± 1.88	52.53 ± 5.17	p = 0.403	1.09 ± 1.35	96.98 ± 4.45
Loaded with DS	27.06 ± 2.26	72.93 ± 2.26	74.29 ± 4.48	p = 0.663	1.35 ± 1.15	101.36 ± 5.37
Sig. (p) (Formulation)	p = 0.001	p = 0.001	p = 0.001		p = 0.867	–

DS is dextran sulfate.
TMPs is transmembrane pressures.
SD is standard deviation.
$p < 0.05$ is significant, $p > 0.05$ is not significant, obtained from one way ANOVA test.
[a]assayed.
[b]expected (100-a), derived from the purification curve (Figure 6).
[c]assayed (assayed using the dry recovered mass of the purified nanoparticles).
[d]estimated {100 – (a + c)}.
[e]estimated (a + c).

performed. Empty nanoparticles with dextran sulfate were prepared and purified. The PVA removal profile (Figure 4) and its distribution values (Table 2) for this batch overlapped with the PVA removal profile of the drug loaded nanoparticles containing dextran sulfate. At the same time their filtration flow rates were not significantly different (p = 0.992) compared to the loaded nanoparticle with dextran sulfate (Figure 5). This indicates that the removal of the drug from the formulation did not affect the PVA purification profile.

To further evaluate the role of drug entrapment on the PVA purification pattern, the drug loaded nanoparticles without dextran sulfate were prepared and purified under similar conditions. The PVA removal was also equally sluggish, with an overlapping pattern initially, then marginally increased towards the end of purification curve (Figure 4). The filtration flow rates were not significantly different (p = 0.608, 0.460) from the empty and loaded nanoparticles containing dextran sulfate (Figure 5, Table 6). This indicates that in the presence of the drug, PVA purification behavior was marginally better compared to purification behavior in the presence of dextran sulfate. Combining these outcomes it is clear that the presence of the dextran sulfate and loperamide HCl reduced the PVA removal rate compared to that of empty nanoparticles without dextran sulfate. The particle sizes of the nanoparticles with

TABLE 4
Impact of Purification on Physical Properties of the Nanoparticle Formulation

Formulations	Particle Size (nm)		Zeta Potential (mV)	
	Before Purification	After Purification	Before Purification	After Purification
Nanoparticle Formulation-sodium cholate as a surfactant (w/o/w)				
No drug (10 psi)	273.10 ± 14.80	271.20 ± 17.40	–	–
No drug (20 psi)	290.50 ± 13.40	290.40 ± 11.00	–	–
Nanoparticle formulation – PVA as a surfactant (o/w)				
Empty without DS (20 psi) (n = 3)	108.50 ± 7.58	102.20 ± 2.05	−10.30 ± 1.60	−20.58 ± 3.65
Loaded without DS (20 psi) (n = 3)	109.00 ± 5.06	100.90 ± 3.76	−0.4 ± 1.30	−8.4 ± 1.93
Loaded with DS (20 psi) (n = 3)	109.63 ± 2.75	104.10 ± 2.19	0.19 ± 0.030	1.70 ± 0.26
Empty with DS (20 psi) (n = 1)	106.40	100.25	−15.02	−12.3

TABLE 5
Impact of the Transmembrane Pressure on Mean Filtrate Flow Rate

Mean Filtration Flow Rate (mL/min) (n = Time Points Used in the Flow Rate Determination)		
	Transmembrane Pressure	
Formulation Type	10 psi	20 psi
The empty nanoparticles suspension containing sodium cholate as a surfactant	1.89 ± 0.04 (n = 8)	2.63 ± 0.06 (n = 8)

Mean flow rate at 20 psi was significantly higher (p = 0.000) compared to 10 psi.

$p < 0.05$ is significant, $p > 0.05$ is not significant, obtained from one way ANOVA test.

TABLE 6
Statistical Comparison of the Mean Flow Rates Obtained from Purification of the Nanoparticles Formulations Containing PVA on TFF at 20 psi Transmembrane Pressure

Mean Flow Rate (mL/min) (n = Time Point Used in the Flow Rate Determination)		
Formulation Type	Flow rate Comparison	Sig. (p)
Empty without DS	Loaded without DS	0.039
3.71 ± 0.44 (n = 11)	Loaded with DS	0.005
	Empty with DS	0.007
Loaded without DS	Empty without DS	0.039
2.73 ± 0.42 (n = 16)	Loaded with DS	0.460
	Empty with DS	0.608
Loaded with DS	Empty without DS	0.005
2.28 ± 0.15 (n = 16)	Loaded without DS	0.460
	Empty with DS	0.992
Empty with DS	Empty without DS	0.007
2.36 ± 0.18 (n = 16)	Loaded without DS	0.608
	Loaded with DS	0.992

Mean flow rate value was calculated separately for each formulation, from each time point value of average curve in Figure 5 after excluding initial five readings.

Sig. (p) values were obtained from the one way ANOVA comparison, with Scheffe's post hoc test.

$p < 0.05$ is significant, $p > 0.05$ is not significant.

dextran sulfate and without dextran sulfate were almost similar, thus removing the possibility of a size involvement in the retardation of PVA removal. In various preparations of the nanoparticles overall surface charges ranged from neutral to negative values, which is less likely to affect the negatively charged polyether sulfone membrane of the TFF cassette in reducing the flow rate. From their zeta potential values (Table 4), it was not possible to derive any correlation between the reduced filtrate flow rate and surface charge of the nanoparticles. The reduced flow rate may be explained by the following hypothesis (1) enhanced entrapment of the PVA in the presence of excipient and drug may slow PVA purification rate. (2) Adsorption of the dextran sulfate, a rigid molecule onto the membrane may reduce the passage of the PVA across the membrane hence slow filtrate flow rate. The later reason may contribute to a lesser extent to cause such a slow down in PVA removal, because when dextran sulfate was removed from the loaded nanoparticle formulation, it still provided sluggish PVA removal, this means dextran sulfate adsorption was not the only reason for the impaired PVA removal. Its adsorption on the membrane might contribute to a marginal reduction in PVA purification performance (Figure 4). The first possibility is more likely and from the above outcomes it was hypothesized that the PVA could be entrapped to a higher extent into the core of the nanoparticle in the presence of drug and dextran

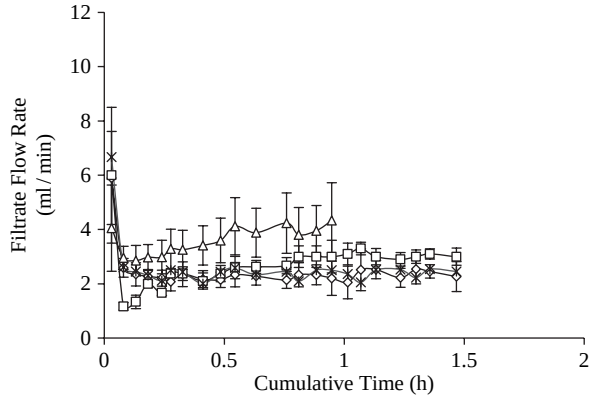

FIGURE 5. Impact of dextran sulfate on the filtrate flow rate at 20 psi. -Δ- empty nanoparticle without drug and without dextran sulfate (n = 3). -✧- loperamide HCL loaded nanoparticles with dextran sulfate (n = 3). -□- loperamide HCL loaded nanoparticles without dextran sulfate (n = 3). -*- empty nanoparticle with dextran sulfate (n = 1). Mean ± *SD* values are derived by excluding initial five time points in above average profiles.

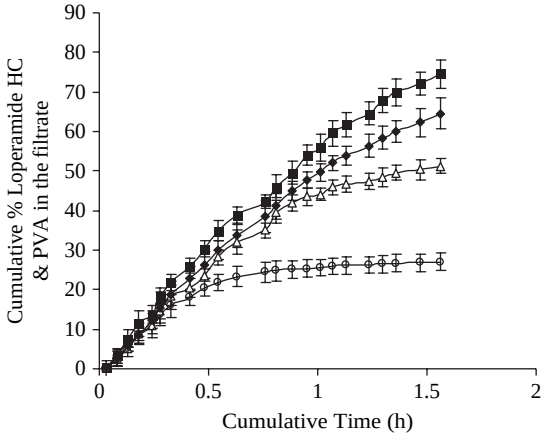

FIGURE 6. Purification of loperamide loaded nanoparticles on TFF at 20 psi transmembrane pressure, comparison of cumulative % pva removed and cumulative % loperamide HCL release. Where, -Δ- loperamide HCl release and -■- PVA removed from the loaded nanoparticle without dextran sulfate. -❍- loperamide HCl release and -✦- PVA removed from the loaded nanoparticle with dextran sulfate.

sulfate compared to their absence. This entrapped PVA is likely to be removed very slowly on dilution, hence leaving higher amounts of PVA associated with nanoparticles. Along with this highly entrapped PVA, its chain is likely to protrude outwards due to high molecular weight (≈9000) and longer chain length compared to a short chain length and comparatively lower molecular weight of PEG_{2000}. This could be dragged towards the surface of the membrane along with nanoparticles during purification and is possibly polarized at the surface which may reduce the filtration flow rate. This was practically reflected in the comparison of the filtrate flow rates for empty and loaded nanoparticles with and without dextran sulfate (Figure 5).

During purification of the drug loaded nanoparticles, free drug was also removed in the filtrate, the loaded nanoparticle without dextran sulfate was observed to have 44.45 ± 1.88%, n = 3 of free drug. In the presence of dextran sulfate only 27.06 ± 2.26%, n = 3 remained as free drug. The difference is believed to be entrapped within the nanoparticles. This was confirmed by assaying the dried weight of recovered nanoparticles, that provided 74.29 ± 4.48%, n = 3 entrapment in the case of loaded nanoparticles with dextran sulfate and 52.53 ± 5.17%, n = 3 entrapment in the case of loaded nanoparticles without dextran sulfate. These were not significantly different (p = 0.663, 0.403) than the expected entrapment efficiencies of the respected formulation derived from the purification curves generated on TFF (Table 3, Figure 6). The presence of the dextran sulfate resulted in increased encapsulation efficiency, possibly due to an ion pairing phenomenon (David, 1997; Meyer, 1995; Powers, 1993).

CONCLUSION

It is clear that in the presence of the drug and other excipients, higher amounts of PVA were associated with nanoparticles that was difficult to remove during purification. As a result, the presence of a rigid molecule like dextran sulfate is likely to increase the d-spacing of the PEG molecules within the stealth on the surface of the nanoparticles. This could potentially disturb the stealth density and allow macrophages to recognize a hydrophobic core for opsonization more quickly, which may result in a reduced half life of such particulate systems. However, the in vivo fate of the proposed nanoparticle system remains to be investigated. From the current study it was clear that, the amount of PVA associated with the empty nanoparticles without dextran sulfate and drug was almost zero, such particles are likely to maintain an ideal stealth surface of the PEG molecules on the nanoparticle, which potentially could be disturbed when incorporation efforts are being made using additional excipients.

ACKNOWLEDGMENT

The authors would like to acknowledge Chemeg Limited for polymer synthesis and characterization supports. Authors would also like to acknowledge Prof. V. B. Sunderland, School of Pharmacy, Curtin University of Technology for reviewing the manuscript and suggesting the technical inputs.

REFERENCES

Beletsi, A., Leontiadis, L., Klepetsanis, P., Ithakissios, D. S., & Avgoustakis, K. (1999). Effect of preparative variables on the properties of poly(dl-lactide-co-glycolide)-methoxypoly(ethyleneglycol) copolymers related to their application in controlled drug delivery. *Int. J. Pharm., 182*(2), 187–197.

Bhatt, M. V., Srinivasan, G., & Neelakantan, P. (1964). On the conformation of cyclohexane 1,4-dione and its derivative-I. Infrared and raman spectra of cyclohexane 1,4-dione and infrared spectrum of its octadeutero analogue. *Tetrahedron, 21*, 291–297.

Charcosset, C. (2006). Membrane processes in biotechnology: An overview. *Biotechnol. Adv., 24*(5), 482–492.

Chiellini, E., Orisini, L. M., & Solaro., R. (2003). Polymeric nanoparticle based on polylactide and related copolymers. *Macromol. Symp., 197*, 345–354.

Child, P., & Rafter, J. (1986). Calcium enhances the hemolytic action of bile salts. Biochim. Biophys. Acta (BBA) - *Biomembranes*, *855*(3), 357–364.

Dailey, L. A., Wittmar, M., & Kissel, T. (2005). The role of branched polyesters and their modifications in the development of modern drug delivery vehicles. *J. Control. Release., 101*(1–3), 137–149.

Dalwadi, G., Benson, H. A., & Chen, Y. (2005). Comparison of diafiltration and tangential flow filtration for purification of nanoparticle suspensions. *Pharm. Res., 22*(12), 2152–2162.

David, Q.-G., Eric, A. m., Hatem, F., & Erie, D. (1997). Applications of the Ion-Pair Concept to Hydrophilic Substances with Special Emphasis on Peptides. *Pharm. Res., V14*(2), 119–127.

Du, Y. J., Lemstra, P. J., Nijenhuis, A. J., Aert, H. A. M., & Bastiaansen., C. (1995). ABA type copolymer of lactide and poly(ethylene glycol). Kinetic, Mechanistic, and Model studies. *Macromolecules*, *28*, 2124–2132.

Durig, J. R. (1963). Far-infrared absorption, vibrational spectra and structure of beta-propiolactone. *Spectrachim. Acta., 19*, 1225–1233.

Durig, J. R., & Morrissey, A. C. (1968). Vibrational spectra and structure of small-ring compond. XI. b-butyrolactone. *J. Mol. Struct., 2*, 377–390.

Finely, J. H. (1961). Spectrophotometric determination of polyvinyl alcohol in paper coatings. *Anal. Chem., 33*, 1952–1957.

Gilding, D. K., & Reed, A. M. (1979). Biodegradable polymers for use in surgery--polyglycolic/poly(actic acid) homo- and copolymers: 1. *Polymer*, *20*(12), 1459–1464.

Govender, T., Stolnik, S., Garnett, M. C., Illum, L., & Davis, S. S. (1999). PLGA nanoparticles prepared by nanoprecipitation: drug loading and release studies of a water soluble drug. *J. Control. Release., 57*(2), 171–185.

Gref, R., Domb, A., Quellec, P., Blunk, T., Muller, R. H., Verbavatz, J. M., et al. (1995). The controlled intravenous delivery of drugs using PEG-coated sterically stabilized nanospheres. *Adv. Drug Del. Rev. Long-circulating Drug Delivery Systems, 16*(2–3), 215–233.

Guichardon, P., Moulin, P., Tosini, F., Cara, L., & Charbit, F. (2005). Comparative study of semi-solid liposome purification by different separation methods. *Sep. Purif. Technol., 41*(2), 123–131.

Heydenreich, A. V., Westmeier, R., Pedersen, N., Poulsen, H. S., & Kristensen, H. G. (2003). Preparation and purification of cationic solid lipid nanospheres-effects on particle size, physical stability and cell toxicity. *Int. J. Pharm., 254*(1), 83–87.

Kim, D., El-Shall, H., Dennis, D., & Morey, T. (2005). Interaction of PLGA nanoparticles with human blood constituents. Colloids Surf. B: *Biointerfaces, 40*(2), 83–91.

Kister, G., Cassanas, G., Fabregue, E., & Bardet, L. (1992). Vibrational analysis of ring opening polymerization of glycolide, L-lactide and D,L-lactide. *Eur. Polym. J., 28*, 1273–1277.

Limayem, I., Charcosset, C., & Fessi, H. (2004). Purification of nanoparticle suspensions by a concentration/diafiltration process. *Sep. Purif. Technol., 38*(1), 1–9.

Meyer, J. D., James E. Matsuura, Brent S. Kendrick, Emily S. Evans, Gabriel J. Evans, & Mark C. Manning. (1995). Solution behavior of α-chymotrypsin dissolved in nonpolar organic solvents via hydrophobic ion pairing. *Biopolymers, 35*(5), 451–456.

Mosbach, E. H., Kalinsky, H. J., Halpern, E., & Kendall, F. E. (1954). Determination of deoxycholic and cholic acids in bile. *Arch. Biochem., 51*(2), 402–410.

Mu, L., & Feng, S. S. (2002). Vitamin E TPGS used as emulsifier in the solvent evaporation/extraction technique for fabrication of polymeric nanospheres for controlled release of paclitaxel (Taxol$^{(R)}$). *J. Control. Release., 80*(1–3), 129–144.

Murakami, H., Kobayashi, M., Takeuchi, H., & Kawashima, Y. (1999). Preparation of poly(D,L-lactide-co-glycolide) nanoparticles by modified spontaneous emulsification solvent diffusion method. *Int. J. Pharm., 187*(2), 143–152.

Niwa, T., Takeuchi, H., Hino, T., Kunou, N., & Kawashima, Y. (1993). Preparations of biodegradable nanospheres of water-soluble and insoluble drugs with -lactide/glycolide copolymer by a novel spontaneous emulsification solvent diffusion method, and the drug release behavior. *J. Control. Release., 25*(1–2), 89–98.

Olivier, J.-C., Huertas, R., Lee, H. J., Calon, F., & Pardridge, W. M. (2002). Synthesis of Pegylated Immunonanoparticles. *Pharm. Res., 19*(8), 1137–1143.

Powers, M., Matsuura, J., Brassell, J., Manning, M. C., & Shefter, E. (1993). Enhanced solubility of proteins and peptides in nonpolar solvents through hydrophobic ion pairing. *Biopolymers, 33*(6), 927–932.

Quintanar-Guerrero, D., Fessi, H., Allemann, E., & Doelker, E. (1996). Influence of stabilizing agents and preparative variables on the formation of poly(-lactic acid) nanoparticles by an emulsification-diffusion technique. *Int. J. Pharm., 143*(2), 133–141.

Reis, R., Gadam, S., Frautchy, L. N., Otlando, S., Goodrich, E. M., Saksena, S., et al. (1997). High performance tangential flow filtration. *Biotechnol. Bioeng., 56*, 71–82.

Riley, T., Govender, T., Stolnik, S., Xiong, C. D., Garnett, M. C., Illum, L., et al. (1999). Colloidal stability and drug incorporation aspects of micellar-like PLA-PEG nanoparticles. Colloids Surf. B: *Biointerfaces, 16*(1–4), 147–159.

Sahoo, S. K., Panyam, J., Prabha, S., & Labhasetwar, V. (2002). Residual polyvinyl alcohol associated with poly (,-lactide-co-glycolide) nanoparticles affects their physical properties and cellular uptake. *J. Control. Release., 82*(1), 105–114.

Sweeney, S. F., Woehrle, G. H., & Hutchison., J. H. (2006). Rapid purification and size separation of gold nanoparticles via diafiltration. *J. Am. Chem. Soc., 128*, 3190–3197.

Tishchenko, G., Hilke, R., Albrecht, W., Schauer, J., Luetzow, K., Pientka, Z., et al. (2003). Ultrafiltration and microfiltration membranes in latex purification by diafiltration with suction. *Sep. Purif. Technol., 30*(1), 57–68.

Vandervoort, J., & Ludwig, A. (2002). Biocompatible stabilizers in the preparation of PLGA nanoparticles: a factorial design study. *Int. J. Pharm., 238*(1–2), 77–92.

Youan, B. C., Hussain, A., & Nguyen, N. T. (2003). Evaluation of sucrose esters as alternative surfactant in microencasulation of proteins by the solvent evaporation method. *AAPS PharmSci., 5*(2), 1–9.

ADDITIONAL REFERENCES

Allémann, E., Doelker, E. and Gurny R. 1993. Drug loaded poly(lactic acid) nanoparticles produced by a reversible salting out process: Purification of an injectable dosage form. Eur. J. Pharm. Biopharm. 39 (1) 13–18.

Spalla, O. 2002. Nanoparticle interaction with polymers and polyelectrolytes. Current. Opinion in Colloid and Interface Science. (7) 179–185.